General Disclaimer

One or more of the Following Statements may affect this Document

- This document has been reproduced from the best copy furnished by the organizational source. It is being released in the interest of making available as much information as possible.

- This document may contain data, which exceeds the sheet parameters. It was furnished in this condition by the organizational source and is the best copy available.

- This document may contain tone-on-tone or color graphs, charts and/or pictures, which have been reproduced in black and white.

- This document is paginated as submitted by the original source.

- Portions of this document are not fully legible due to the historical nature of some of the material. However, it is the best reproduction available from the original submission.

NASA TECHNICAL MEMORANDUM

NASA TM X-73683

NASA TM X-73683

THEORETICAL AND EXPERIMENTAL STUDIES OF THE DEPOSITION OF Na_2SO_4 FROM SEEDED COMBUSTION GASES

by Fred J. Kohl, Gilbert J. Santoro,
Carl A. Stearns, and George C. Fryburg
Lewis Research Center
Cleveland, Ohio 44135

and

Daniel E. Rosner
Department of Engineering and Applied Science
Yale University, New Haven, Connecticut 06520

TECHNICAL PAPER presented at the
Symposium on Corrosion Problems Involving Volatile Corrosion Products
sponsored by the Electrochemical Society
Philadelphia, Pennsylvania, May 8-13, 1977

THEORETICAL AND EXPERIMENTAL STUDIES OF THE DEPOSITION OF Na_2SO_4 FROM SEEDED COMBUSTION GASES

by Fred J. Kohl, Gilbert J. Santoro, Carl A. Stearns,
and George C. Fryburg
NASA Lewis Research Center
Cleveland, Ohio 44135
and
Daniel E. Rosner
Department of Engineering and Applied Science
Yale University, New Haven, Connecticut 06520

E-9031

ABSTRACT

The deposition of sodium sulfate from flames containing sodium and sulfur is regarded as one of the fundamental steps in the phenomenon of "hot corrosion" of turbine components. Recently, a local thermochemical equilibrium (LTCE) method of predicting condensation temperatures of sodium sulfate in flame environments was described. This paper presents results of an experimental study to test the validity of the theoretical dew point predictions and to provide the basis for developing a deposition rate theory. Experiments were run in a Mach 0.3 atmospheric pressure laboratory burner rig. Flames were doped with sea salt, Na_2SO_4, and NaCl, respectively. Deposits were collected on cylindrical platinum targets placed in the combustion products, and the deposition was studied as a function of collector temperature. Experimental deposition onset temperatures checked within experimental error with LTCE-predicted temperatures. A multicomponent mass transfer equation was developed to predict the rate of deposition of $Na_2SO_4(c)$ via vapor transport at temperatures below the deposition onset temperature. The phenomena of species transport by simultaneous Fick diffusion, Soret (thermal) diffusion, convection and turbulence are included, subject to the basic assumption that no reaction or phase change occur

STAR Category 26

within the vapor diffusion boundary layers. Agreement between maximum deposition rates predicted by this chemically frozen boundary layer (CFBL) theory and those obtained in the seeded laboratory burner experiments is good, but the predicted dependence on surface temperature exhibits plateau like behavior not evident in the present experimental results.

INTRODUCTION

The deposition of sodium sulfate from flames containing sodium and sulfur is regarded as one of the fundamental steps in the phenomenon of hot corrosion on turbine components. The presence of sulfur in fuels and the ingestion of various inorganic salts into combustion chambers along with intake air have been related to instances of hot corrosion attack in marine, industrial, and aircraft turbine engines. Because Na_2SO_4 is the major phase recovered from the turbine surfaces, an equilibrium thermodynamic description of the fate of sodium and sulfur and other elements leading to the formation of condensed Na_2SO_4 is useful in understanding the initial important stages of the corrosion mechanism.

Recently, we described (ref. 1) an equilibrium thermodynamic method of predicting condensation onset temperatures (dew points) of Na_2SO_4 in flame environments as a function of sulfur and sea salt concentration in the fuel and intake air, respectively. The method consisted of applying the widely used NASA computer program (ref. 2) for calculating equilibrium flame compositions and temperatures. The thermodynamic properties of gaseous and condensed phase Na_2SO_4, along with additional species pertinent in sea salt-containing environments, were used in the program to calculate equilibrium flame compositions and temperatures for representative turbine engine and burner rig flames. Compositions were calculated at various fuel-to-oxidant ratios with different additions of sulfur to the fuel and of sea salt to the

intake air. Temperatures were specified for which condensation of Na_2SO_4 should be expected.

This paper describes the results of an experimental study employing a burner rig to test the validity of the theoretical dew point predictions. The burner flame was doped with roughly 10 ppm of an inorganic salt containing sodium (sea salt, Na_2SO_4, or NaCl), and deposits were collected on a platinum cylinder situated in the flame. The deposition rate was determined at different collector temperatures. It was anticipated that if the predictions were accurate for a burner rig environment, this result would lend credence to predictions for actual engine conditions, and to specifications for operating parameters necessary for realistic burner rig simulation of engine conditions.

During the course of this research, it became obvious that a theoretical prediction was desirable for the rates of deposition of $Na_2SO_4(c)$ at temperatures below the deposition onset temperature. A mass transfer equation was developed for these predictions, and is compared with results for Na_2SO_4-seeded flames.

EXPERIMENTAL

Description of Apparatus

Mach 0.3 burner rig. - The burner of the Mach 0.3 rig (fig. 1) consisted of a nozzle with a 2.54 cm diameter throat made of the cobalt base alloy, L605; a burner housing; a backplate; and a burner can or lining. The housing was fitted with a fire-eye (a safety feature which automatically shuts off the fuel supply should the flame be extinguished), an ignitor to initiate combustion, and an aspirator-type feed for aqueous salt solution injection. The aspirator tube was located 12.3 cm downstream of the ignitor. The salt solution was fed to the aspirator by a peristaltic pump which was set at 200 cc/hour and a discharge pressure of 40 psi. The liner of the burner housing was fitted with a swirl plate

such that the fuel was fed through a nozzle in the center of the swirl plate and air was fed through many angularly drilled holes in the swirl plate around the fuel nozzle. This swirl plate was fitted against the backplate of the burner housing on which were attachments for the fuel and the air lines.

The fuel (Jet A-1, ASTM D-1655) was pumped from a large storage tank outside the building and an aliquot of the fuel supply for analysis was taken each time the tank was refilled. The fuel samples were analyzed for sulfur by a Parr bomb calorimeter combustion technique. The sulfur content of the fuel ranged from 0.021 to 0.068 percent. The fuel flow to the burner and the air flow were metered by calibrated rotameters. The inlet temperature of the fuel was 298 K and the rig was operated at one atmosphere pressure. A typical fuel/air mass ratio was 0.04. Flame temperature was monitored by a controlling optical pyrometer.

A characteristic of the burner that was important in this study was the residence time of the dopant in the flame; i.e., the time interval between introduction of dopant into the burner and arrival at the platinum collector. Calculations revealed that the residence time was 2.2 msec.

Collector Assembly. - The collector assembly (fig. 1(b) and 2) consisted of a collector, collector support and its stem, and a base. The collector was made of a platinum-10-percent rhodium thin walled tube with slightly tapered walls. Its height was 1.27 cm and the diameter of its base was 1.27 cm. The small size of the collector was chosen to facilitate temperature uniformity over the entire surface when placed in the burner flame. The collector was mounted snugly over the collector support. The collector support was hollow with a closed top, and had a tube (stem) 0.64 cm in diameter fitted at its base. The support and its stem were made of Inconel (IN-600). Around the stem between the support and the base was a loose fitting Al_2O_3 tube that acted as a thermal barrier for the stem and prevented hot corrosion of the stem. The junction of a chromel-alumel thermocouple was

peened in a hole in the wall of the collector support, 0.64 cm from its base. The thermocouple leads extended through the support and its stem, out of the stainless steel collector base, and were attached to a slip ring electrical contact. The thermocouple's output was recorded. The stem of the collector support was secured to the collector base by a set screw. The base, in turn, was attached by set screws to the shaft of a variable speed motor that rotated the entire collector assembly at about 100 rpm to assure temperature uniformity.

Test Procedures

Tests run. - Four series of tests were performed, each with different dopants, but in all cases the level of sodium by weight in the air was roughly the same, about 3.4 ppm:

1. Sea salt - about 11.3 ppm - see composition, table I, part A.
2. Na_2SO_4 - about 10.5 ppm - reagent grade.
3. NaCl - about 8.0 ppm - reagent grade.
4. NaCl + CS_2 addition to the fuel - about 8.0 ppm salt and total sulfur content of fuel about 0.25 wt percent.

Burner rig operation. - All testing followed this procedure. The collector was ultrasonically cleaned in ethyl alcohol, dried, weighed, and mounted on the collector support. The burner gases were ignited and controls were adjusted for a stable flame. Fuel and air flows were approximately set. The burner was rotated into the heating position and the temperature of the collector was monitored by the thermocouple and an optical pyrometer. The burner controls were adjusted to obtain the desired collector temperature. When a steady flame and the correct temperature were obtained (within 10 minutes), the salt was turned on. The temperature and burner controls were monitored at 10-to-20 minute intervals and adjustments were made as needed to maintain collector temperature. Fuel and air flows were manually recorded. After 6 hours at temperature, the burner was rotated to the cool position and turned

off. After the collector cooled, it was taken from its support, weighed and submitted for analysis of its deposit. After each run, the burner was disassembled and cleaned of carbon and salt deposits.

An exception to this operation was the test conducted at 700° C. To reach this low temperature, cooling air was added to the flame in the burner. This air flow was not measured, so the fuel/air ratios could not be determined.

Analysis of deposits. - Water soluble salts were leached from collectors by treating with warm water for 1/2 hour. Acid soluble salts were dissolved by leaching with 1:1 HCl for a subsequent 1/2 hour. The two solutions obtained from the leachings were analyzed for the components of sea salt: Na^+, K^+, Ca^{++}, Mg^{++}, $SO_4^=$, and Cl^-. The metal cations were determined by atomic absorption. The $SO_4^=$ was determined by the X-ray fluorescence method of Luke (ref. 3), modified to allow precipitation times of 5 hours or longer because of the larger amounts of sulfate involved. Tests for Cl^- were made by the mercuric thiocyanate method (ref. 4).

LOCAL THERMOCHEMICAL EQUILIBRIUM THEORY

Previously we have calculated compositions of combustion gases and Na_2SO_4 condensation onset temperatures for typical sea-salt doped turbine engine and burner rig flames (ref. 1). To analyze the present series of burner rig experiments, similar calculations were made for the specific conditions employed here. The various input parameter and typical results are shown in table I.

Calculations were performed with the NASA complex chemical equilibrium computer program (ref. 2) which has been described previously. This program is based on the minimization of free energy approach to chemical equilibrium calculations subject to the constraint of maintaining a proper mass balance between reactants and products. The program permits the calculation of chemical equilibrium composition for homogeneous or heterogeneous systems for assigned thermodynamic states such as temperature-pressure (T, P) and enthalpy-pressure (H, P).

DEPOSITION RATE THEORY

Approach and Objectives

The experimental data reported in this paper provide a useful basis for developing and validating a deposition rate theory. A tractable theoretical model sufficiently general to explain observed deposition rates from the present burner rig gases would be promising for application under gas turbine conditions.

The experimental existence of a "dew point" surface temperature above which no deposition of $Na_2SO_4(c)$ was observed suggested that deposition was associated with vapor diffusion to the collector across a gaseous diffusion "boundary layer." Accordingly, a convective diffusion theory for predicting Na_2SO_4 deposition rates in the burner rig experiments has been developed (ref. 5). To proceed, based on readily available information, we make the following two simplifying assumptions: (1) all sodium added to the combustion gases is available for transport to the target via vapor species, and (2) while local thermochemical equilibrium (LTCE) is achieved at the outer and inner edges of the concentration boundary layer around the collector, no homogeneous chemical reactions occur within the diffusion boundary layer.[1] In contrast to previous treatments of vapor deposition (ref. 7) provision is here made for the effects of: (a) Na-element transport via species of differing mobility (i.e., NaOH(g), Na(g), $Na_2SO_4(g)$), (b) thermal diffusion of heavy, Na-containing species and (c) free stream turbulence intensity and scale.

---

[1] A boundary layer in which homogeneous chemical reactions are negligible is said to be chemically "frozen" (CF). The opposite extreme of chemical reactivity is that of local thermochemical equilibrium (LTCE) everywhere (not only at stations e, w). A tractable deposition rate theory under LTCE conditions is presently under investigation (ref. 6).

While condensed Na_2SO_4 can be formally regarded as one of the diffusing "species," in practice our knowledge of the particle size distribution (hence Brownian and thermophoretic diffusion parameters) is presently inadequate to assess this contribution to the observed deposition rate. For this reason only vapor diffusion is included in the preliminary boundary layer predictions discussed below. Nevertheless, predicted maximum deposition rates will be shown to agree to within experimental error with rates observed for Na_2SO_4 addition experiments. We conclude with a discussion of necessary extensions of the present chemically frozen boundary layer (CFBL) theory to account for deposition rate over-predictions very near, and far below, the dew point.

Formulation

We consider the deposit collected per unit time to be the resultant of the transport of each sodium-containing species i ($i = Na_2SO_4(g)$, NaOH(g), Na(g), . . .) present in the local gas mixture with time-average mass fraction ω_i (with $\omega_i << 1$). If $\dot{m}_i''$ is the corresponding deposition flux for species i then the deposition flux for the chemical element sodium (Na), irrespective of its state of combination, is

$$\dot{m}''_{(Na)} = \sum_i \omega_{Na/i} \dot{m}_i'' \qquad (1)$$

where the weighting factor $\omega_{Na/i}$ denotes the mass fraction of molecule i comprised of element Na. Because the deposit is predominantly $Na_2SO_4(c)$ the total deposition flux can then be written $\dot{m}''_{(Na)}/\omega_{Na/Na_2SO_4}$, where $\omega_{Na/Na_2SO_4} = 0.3237$.

Our expressions for the $\dot{m}_i''$ must take into account the simultaneous processes of Fick (concentration) diffusion, Soret (thermal) diffusion, convection and turbulence within the gaseous boundary layer enveloping

the target. The first two phenomena are characterized by the transport coefficients D_i (Fick diffusivity) and α_i (thermal diffusion factor) appearing in the diffusional mass flux law:

$$j_i'' = -(D_i\rho)(\nabla\omega_i + \alpha_i\omega_i\nabla \ln T) \tag{2}$$

In the absence of thermal diffusion we know from abundant previous experience that each CFBL convective diffusion mass flux can be conveniently written in the separable form:

$$\dot{m}_i''(\text{CFBL}, \alpha_i = 0) = \frac{(D_i\rho)_e}{L} \cdot F(\text{turb}) \cdot Nu_{m,i}(Re, Sc_i, \ldots) \cdot (\omega_{i,e} - \omega_{i,w}) \tag{3}$$

where

$Nu_{m,i}$ ≡ dimensionless mass transfer (Nusselt or Sherwood) coefficient (essentially defined by eq. (3))

L ≡ characteristic body length associated with $Nu_{m,i}$

Re ≡ Reynolds number for the local viscous flow

Sc_i ≡ ν/D_i (Kinematic-to-Fick diffusivity ratio)

$F(\text{turb})$ ≡ correction factor for effect of free stream turbulence level and scale

$\omega_{i,e} - \omega_{i,w}$ ≡ "driving force" for species i Fick diffusion across the boundary layer (edge e, wall w)

We have recently shown (refs. 5, 8) that the inclusion of thermal diffusion introduces two effects; viz.

(a) A convection-like (thermophoretic) term in the species i conservation equation, which produces a "suction-like" augmentation of the mass transfer coefficient $Nu_{m,i}$ by the factor $F(\text{Soret})$.

(b) A non-Fick contribution to the species i flux at the wall (whenever $\omega_{i,w}$ is nonzero).

If we then write $F(\text{Soret}) = F(\tau_i, Le_i, \ldots)$, where:

$$\tau \equiv \alpha_{i,w}(Le_{i,w})^{0.4}[(T_e - T_w)/T_w] \quad \text{(thermophoretic parameter)}^2 \quad (4)$$

$$Le_i \equiv D_i/[\lambda/(\rho c_p)] \quad \text{(Fick-to-thermal diffusivity ratio)} \quad (5)$$

each $\dot{m}_i''$ can be expressed (refs. 5, 8):

$$\dot{m}_i'' = \frac{(D_i\rho)_e}{L} \cdot F(\text{turb})F(\tau_i, Le_i, \ldots) \cdot Nu_{m,i} \cdot \left[(\omega_{i,e} - \omega_{i,w}) + \frac{\tau_i}{F(\tau_i, Le_i, \ldots)} \cdot \omega_{i,w}\right] \quad (6)$$

The predictions below are based on equations (1, 6) averaged over the wetted perimeter of the target in cross flow.

Specific Assumptions and Input Data

To implement this approach using the burner rig and LTCE Computer Code information cited earlier, we assumed:

(a) The adiabatic combustion temperature is equivalent to the stagnation temperature T_e^o at the collector location.

(b) The linear velocity of the gas mixture at the collector location is based on that expected from one-dimensional gas dynamics, corrected for the effect of jet exit velocity profile shape (using pipe flow information) and flow divergence (the predictions below are based on no further spread downstream of exit plane).[3]

---

[2]If the free stream Mach number is not negligible then T_e should be replaced by the gasdynamic "recovery" temperature.

[3]Since the "core" length in a turbulent axisymmetric free jet (cf. fig. 1) is about 4.4 jet diameters, the collector is within this core and no further reduction factor is necessary.

(c) All gas properties (density, viscosity, thermal conductivity (λ), etc.) are appropriate to the prevailing mixture of perfect gases. Transport properties were based on Lennard-Jones (12:6)-parameters taken from Svehla's compendium (ref. 9) or estimated using similar procedures (e.g., $Na_2SO_4(g)$). Mixture transport properties were computed from species values via simple (Wassiljewa-type) mixing rules.

(d) Thermal diffusion factors α_i were predicted from estimated Lennard-Jones 12:6 potential parameters based on Chapman-Enskog theory (ref. 10), in the dilute gas ($\omega_i << 1$) limit.

(e) Turbulence intensity and axial macroscale at the collector location were estimated to be about 2.6 pct and 1.63 cm, respectively (ref. 11); the experimental results of ref. 12 were used to assess the influence of these free-stream turbulence parameters on time-averaged transport rates to the collector with resulting F(turb) values being typically 1.16-1.18.

(f) By making the replacement $Pr \rightarrow Sc_i$, the mass transfer coefficient $Nu_{m,i}$ was based on the (arithmetic) mean between heat transfer correlations recommended for stationary infinite circular cylinders, and spheres (ref. 13).[4] At the prevailing target spin rates, no further augmentation of transfer coefficient is required (ref. 14).

(g) Gas compositions (ω_i) at the inner (wall) edge of the boundary layer are not very different from those predicted by the NASA-

---

[4]While the collector (cf. fig. 2) was a "truncated" cylinder (rather than an infinite cylinder or sphere), the dominance of the Re-dependent terms in $Nu_{m,i}(Re, Sc_i, \ldots)$, which are common to both extreme geometries, suggests that this approximation to $Nu_{m,i}$ is adequate for present purposes. For $i = Na_2SO_4$ we found $Sc_i \approx 1.77$ and $Nu_{m,i}$ took on values between 70.6 and 80.5.

LTCE Code (cf. refs. 1, 2 and table I), without allowing for element separation by thermal diffusion.[5]

(h) The perimeter-mean suction function F(Soret) can be estimated from the film (Couette-flow) theory result: $\tau_{eff}/[1 - \exp(-\tau_{eff})]$, where τ_{eff} incorporates τ (eq. (4)) and the influence of variable properties in the vapor concentration sublayer (ref. 8) when Le_i is non-zero.

EXPERIMENTAL RESULTS

Preliminary Tests

Blank runs were made without salt additions to the flame to ascertain if any extraneous sources of deposits existed. None were discovered; i.e., no weight gains greater than 0.05 mg h^{-1} were recorded.

A series of runs were made to determine if the rate of deposition from doped flames was independent of time. The results for a sea salt-doped flame are presented in figure 3, in which the weight gain observed is plotted against length of time of the run. The weight gain obeys linear kinetics indicating that the rate of deposition is independent of time.

Sea Salt-Doped Flame

The results of the deposition of Na_2SO_4 from sea salt-doped flames are shown in figure 4. The rate of deposition, in mg h^{-1}, is plotted against the collector temperature. The line represents the least squares fit of the experimental points, and extrapolation of the line to zero

---

[5]An iterative correction for such element redistribution (refs. 8, 15) will be included in future applications of the CFBL theory outlined here.

rate of deposition yields a dew point of 1260 K. This compares approximately with the predicted value of 1235 K (±10 K).[6] The discrepancy in the dew point values is probably within experimental error.

Rates of deposition were also obtained for $CaSO_4$ and these results are given in figure 5. Extrapolation of the least squares line (points at 975 and 1075 K not included) yields a dew point of 1295 K that compares with a predicted value of 1335 K (±10 K). The rate of deposition levels off at temperatures about 150° C below the dew point.

Chemical analyses of the water-leached solutions revealed that no soluble Cl^- was present in the deposits above background level. Generally, Na^+, K^+, Ca^{++}, and $SO_4^=$ were found only in water leached solutions. Therefore, mass balances were made on the assumption that the salts present on the collector were Na_2SO_4, K_2SO_4, and $CaSO_4$. The Mg^{++} was found mostly in the acid leached solution, so it was assumed that MgO was present on the collector. These assignments were in agreement with the predictions of the chemical equilibrium computer program (ref. 1).

Frequently, an insoluble residue remained after the acid leach. The residues were examined by inert-arc emission spectrography (ref. 16) and found to consist of Fe with smaller amounts of all the elements found in alloy L605, the material used in the burner rig nozzle.

X-ray diffraction analysis of the deposit from sea salt doped flames indicated that the deposit was composed primarily of an anhydrous form of Na_2SO_4. SEM micrographs of the deposit, figure 6, disclosed that the deposit consisted of crystalline needles protruding from a fibrous mat. EDS spectra showed that the needles were composed mainly of

---

[6]Because of variations in the dopant level, fuel sulfur content, and fuel/air ratio in individual runs, the predicted value of the dew point varied. The value was most sensitive to the sulfur content and least sensitive to the fuel/air ratio. The predicted value given here is an average value for all the runs, and the range specified indicates the amount of variation.

sodium and sulfur, characteristic of Na_2SO_4. The matted areas indicated the presence of small amounts of magnesium and calcium in addition to sodium and sulfur. These areas also exhibited low level contamination by nickel, iron, and chromium, most probably from the nozzle of the burner.

Sodium Sulfate-Doped Flame

Deposition results for Na_2SO_4-doped flames are presented in figure 7. The doping level of elemental sodium was roughly the same as in the sea salt doped runs; namely, 3.4 ppm as compared to 3.5 ppm, respectively. The rates of deposition were around twice that for the sea salt runs at comparable temperature intervals below the dew point. Extrapolation of the least squares fitted line (point at 975 K not included) yielded a value of 1280 K for the dew point. This agreed well with the predicted value of 1280 K ($\pm$5 K).

The data point plotted at 975 K exhibited a large drop in the rate compared with rates at higher temperatures. It is not certain whether this resulted from the effect of the large quantity of cooling air added during this run, or whether it resulted from nucleation and subsequent condensation of Na_2SO_4(g) into particles (ref. 7).

Sodium Chloride-Doped Flame

Deposition rates of Na_2SO_4 were measured for flames doped with NaCl. The level of doping was adjusted to give about the same sodium level as in the sea salt runs; 3.1 ppm as compared with 3.5 ppm. Runs were made with two concentrations of sulfur in the fuel: one, the undoped fuel that contained 0.032 percent sulfur; and another in which CS_2 was added to yield a sulfur concentration of 0.25 percent.

The rates of deposition of Na_2SO_4 are presented in figure 8. Examination of the results discloses that the rates of deposition for the higher sulfur concentration were comparable with those obtained with the sea salt-doped flame. The value of the dew point obtained by extrapolating the least squares line was 1250 K compared with the predicted value of 1265 K (±5 K).

The rates of deposition for the lower concentration of sulfur were lower than those for the higher concentration. The dew point obtained by extrapolating the line drawn between the two points was 1180 K. The predicted value was 1240 K. The large discrepancy probably resulted from experimental error since only three runs were made with the low sulfur concentration, one of which was above the dew point. Therefore, these data do not constitute a valid test of the theory.

X-ray diffraction analysis of the deposit from NaCl-doped flames indicated the presence of an anhydrous form of Na_2SO_4. Chemical analyses of the water leached solutions revealed the absence of any detectable Cl^- above background level. These results demonstrated that NaCl can be converted to Na_2SO_4 in a burner rig combustor in 2.2 msec.

Deposition Rate Predictions

Combining equations (1, 6) with the abovementioned assumptions and using species compositions obtained from the NASA-LTCE Computer Code (ref. 1 and Table I), we predicted the total Na_2SO_4 deposition rates (flux times collector area, with result expressed in mg h^{-1}) shown in figure 9 for the Na_2SO_4 seed experiments.[7] Two predictions are displayed: one based on the assumed absence of thermal diffusion ($\alpha_i = 0$, $\tau_i = 0$, $F_i(\text{Soret}) = 1$) and one based on our estimate of the largest likely τ_{eff}

[7]The linearity of deposit mass with collection time (fig. 3) precludes the role of aerodynamic runoff/stripping in limiting the deposit thickness analyzed herein.

and, hence, F_i(Soret). Note that this CFBL method is reasonably successful in estimating maximum deposition rates far below the dew point, however it apparently overpredicts rates just below the dew point. Put another way, regardless of the role of thermal diffusion, the present CFBL theory does not predict the more gradual (nearly linear) increase of deposition rate with departure from the dew point temperature ($T_{dp} - T_w$) observed experimentally. This also proved to be the case for the seasalt- and NaCl-seeding experiments (not shown in fig. 9).

Pending much-needed improvements in the characterization and precision of the deposition experiments, speculation on necessary refinements in the CFBL theory would clearly be premature. However, parallel work is in progress on a fully LTCE boundary layer theory, along with methods for quantitatively including any Na_2SO_4 condensate formed within the boundary layer. Whether this latter phenomenon can produce perimeter-mean deposition rates as low as shown in figure 9 (one point) below 1000 K remains to be seen (refs. 7, 17).

CONCLUDING REMARKS

Appraisal of these results, excluding the NaCl-doped flame with 0.032 percent sulfur for which there were only two data points, indicates that the local thermochemical equilibrium (LTCE) computer program can successfully predict Na_2SO_4 dew points to within the precision of the present experiments. In addition, analogous predictions for the $CaSO_4$ dew point were equally successful and suggest that the LTCE program would be useful with other condensible inorganic salts.

The convective diffusion theory, based on the assumption of a chemically frozen boundary layer (CFBL), was equally successful in predicting the dew point for Na_2SO_4-seeded combustion gases. This theory utilizes the results of the LTCE computer program, which are based on purely thermodynamic considerations, and imposes the additional effects of mass

transport, both Fick and Soret diffusion. The theory was reasonably successful in estimating maximum Na_2SO_4 deposition rates far below the dew point while apparently slightly overpredicting rates just below the dew point. However, it should be pointed out that the burner-rig was being seeded with Na_2SO_4 at a gram per hour level, and deposition was occurring at a milligram per hour level. In spite of this large attenuation, the agreement between experiment and theory is quite satisfactory.

ACKNOWLEDGEMENTS

In preparing the section on DEPOSITION RATE THEORY one of us (DER) wishes to acknowledge computational assistance and helpful discussions with B. K. Chen and R. Srivastava (cf. refs. 5, 6, and 8 for a more detailed account of this phase of the research).

REFERENCES

1. F. J. Kohl, C. A. Stearns, and G. C. Fryburg in "Metal-Slag-Gas Reactions and Processes," Z. A. Foroulis and W. W. Smeltzer, eds., p. 649, The Electrochem. Soc., Princeton, N. J. (1975).

2. S. Gordon and B. J. McBride, NASA SP-273 (1971).

3. C. L. Luke, Anal. Chim. Acta, 43, 245 (1968).

4. T. M. Florence and Y. J. Farrar, Anal. Chim. Acta, 54, 373 (1971).

5. D. E. Rosner, B. K. Chen, G. C. Fryburg, and F. J. Kohl, "Chemically Frozen Multicomponent Boundary Layer Theory of Salt Deposition Rates from Combustion Gases" (in preparation, Spring 1977).

6. D. E. Rosner, "Local Thermochemical Equilibrium Multicomponent Boundary Layer Theory of Salt Deposition Rates from Combustion Gases," (in preparation, Spring 1977).

7. T. D. Brown, J. Inst. Fuel, 39, 378 (1966).

8. D. E. Rosner, and R. Srivastava, "Correlation of Thermal Diffusion Effects on Laminar Boundary Layer Mass Transport Rates" (in preparation, Spring 1977).

9. R. A. Svehla, NASA TR R-132 (1962).

10. J. O. Hirschfelder, C. F. Curtiss, and R. B. Bird, "Molecular Theory of Gases and Liquids," J. Wiley and Sons, New York (1954).

11. J. Laufer, NACA TR-1174 (1954).

12. G. B. Van der Hegge Zijnen, Appl. Sci. Res., A7, 204 (1958).

13. S. Whitaker, Am. Inst. Chem. Eng., 18, 361 (1972).

14. W. M. Kays and I. S. Bjorklund, Trans. Am. Soc. Mech. Eng., 80, 70 (1958).

15. D. E. Rosner, "Effects of Thermal Diffusion on Deposition Rates and Dew Point Predictions in Salt Containing Combustion Gases", (in preparation, Spring 1977).

16. W. A. Gordon and G. B. Chapman, Spectrochim. Acta, 25B, 123 (1970).

17. D. E. Rosner and M. Epstein, J. Colloid Interface Sci., 28, 60 (1968).

Table I. - Thermodynamic Analysis Via Computer Program of Burner Rig Combustion Gases (Ref. 2)

(A) Program Input

Fuel composition: Jet A, $CH_{1.9815}$ (ASTM D-1655), $\Delta H_{298} = -5300$ cal/mol

Sulfur content of fuel: Variable

(a) Sea-salt runs, 0.021 - 0.068 wt.%

(b) Na_2SO_4 runs, 0.021-0.032 wt.%

(c) NaCl runs, 0.032 and 0.25 wt.% (CS_2 added to fuel)

Fuel inlet temperature: 298 K

Composition of air: $N_{1.56176}O_{0.41959}Ar_{0.009324}C_{0.000300}$, $\Delta H_{298} = -28.2$ cal/mol

Moisture in air: one weight percent (approx. 50% relative humidity at 298 K).

Salt concentration: Variable

(a) Sea-salt runs, average 11.3 ppm (wt. in air) $\approx$ 3.5 ppm Na

Sea salt composition

Compound	Wt. percent
NaCl	68.78
$MgCl_2$	14.57
Na_2SO_4	11.46
$CaCl_2$	3.25
KCl	1.93

These are the five most abundant inorganic salts which make up ASTM-D-1141 standard substitute ocean water

(b) Na_2SO_4 runs, average 10.5 ppm (wt. in air) $\approx$ 3.4 ppm Na

(c) NaCl runs, average 8.0 ppm (wt. in air) $\approx$ 3.1 ppm Na

Pressure: one atmosphere

Pressure: One atmosphere
Air inlet temperature: 298 K
Fuel-to-air mass ratio: Variable, ranged from 0.031 to 0.050
Chemical species considered: Over 150 gaseous and condensed species made up of CHNOSCl and Na-, Mg-, Ca-, and K-CHNOSCl combinations

(B) Program Output for typical sea-salt-, Na_2SO_4-, and NaCl-doped flames

(a) Sea-salt-doped flame

Specific input parameters: fuel/air mass ratio = 0.0448; percent sulfur in fuel = 0.038; 11.3 ppm sea salt in air
Calculated adiabatic flame temperature = 1801 K
Calculated Na_2SO_4 dew point = 1235 K

Product Concentrations (mole fraction)

Temperature	T_{flame} = 1801 K	$T_{collector}$ = 1173 K
Species		
Ar(g)	8.78×10^{-3}	8.79×10^{-3}
CO(g)	7.14×10^{-5}	3.10×10^{-9}
CO_2(g)	8.87×10^{-2}	8.88×10^{-2}
$Ca(OH)_2$(g)	9.11×10^{-8}	4.60×10^{-13}
$CaSO_4$(s)	---------	9.12×10^{-8}
H(g)	1.65×10^{-6}	6.16×10^{-12}
HCl(g)	4.06×10^{-6}	3.30×10^{-6}
H_2(g)	2.13×10^{-5}	2.77×10^{-9}
H_2O(g)	9.99×10^{-2}	1.00×10^{-1}
KCl(g)	1.23×10^{-8}	7.56×10^{-8}
KOH(g)	6.67×10^{-8}	3.39×10^{-9}
MgO(s)	---------	4.78×10^{-7}
$Mg(OH)_2$(g)	4.75×10^{-7}	4.39×10^{-11}
NO(g)	2.39×10^{-3}	9.51×10^{-5}
NO_2(g)	3.14×10^{-6}	1.00×10^{-6}

$N_2(g)$	7.34×10^{-1}	7.36×10^{-1}
Na(g)	2.61×10^{-7}	8.87×10^{-12}
NaCl(g)	5.66×10^{-7}	1.50×10^{-6}
NaO(g)	1.30×10^{-8}	1.05×10^{-12}
NaOH(g)	3.33×10^{-6}	6.87×10^{-8}
$Na_2SO_4(l)$	---------	1.25×10^{-6}
$Na_2SO_4(g)$	1.16×10^{-13}	4.63×10^{-8}
O(g)	3.11×10^{-5}	3.57×10^{-9}
OH(g)	5.04×10^{-4}	1.48×10^{-6}
$O_2(g)$	6.51×10^{-2}	6.63×10^{-2}
$SO_2(g)$	1.48×10^{-5}	1.25×10^{-5}
$SO_3(g)$	3.99×10^{-8}	1.04×10^{-6}

(b) Na_2SO_4-doped flame

Specific input parameters: fuel/air mass ratio = 0.0442; percent sulfur in fuel = 0.021; 10.5 ppm Na_2SO_4 in air

Calculated adiabatic flame temperature = 1785 K

Calculated Na_2SO_4 dew point = 1279 K

Product Concentrations (mole fraction)

Temperature	T_{flame} = 1785 K	$T_{collector}$ = 1173 K
Species		
Ar(g)	8.79×10^{-3}	8.79×10^{-3}
CO(g)	5.90×10^{-5}	3.02×10^{-9}
$CO_2(g)$	8.76×10^{-2}	8.77×10^{-2}
H(g)	1.33×10^{-6}	6.09×10^{-12}
$H_2(g)$	1.79×10^{-5}	2.71×10^{-9}
$H_2O(g)$	9.89×10^{-2}	9.92×10^{-2}
NO(g)	2.30×10^{-3}	9.64×10^{-5}
$NO_2(g)$	3.17×10^{-6}	1.03×10^{-6}
$N_2(g)$	7.35×10^{-1}	7.36×10^{-1}
Na(g)	2.68×10^{-7}	1.14×10^{-11}
NaO(g)	1.37×10^{-8}	1.37×10^{-12}
NaOH(g)	3.80×10^{-6}	8.81×10^{-8}

$Na_2SO_4(g)$	1.47×10^{-13}	4.63×10^{-8}
$Na_2SO_4(l)$	----------	1.95×10^{-6}
O(g)	2.72×10^{-5}	3.62×10^{-9}
OH(g)	4.59×10^{-4}	1.48×10^{-6}
$O_2(g)$	6.69×10^{-2}	6.81×10^{-2}
$SO_2(g)$	9.99×10^{-6}	7.40×10^{-6}
$SO_3(g)$	2.88×10^{-8}	6.25×10^{-7}

(c) NaCl-doped flame

Specific input parameters: fuel/air mass ratio = 0.0396; percent sulfur in fuel = 0.25; 8.0 ppm NaCl in air

Calculated adiabatic flame temperature = 1658 K

Calculated Na_2SO_4 dew point = 1268 K

Product Concentrations (mole fraction)

Temperature	T_{flame} = 1658 K	$T_{collector}$ = 1173 K
Species		
Ar(g)	8.83×10^{-3}	8.83×10^{-3}
CO(g)	1.14×10^{-5}	2.47×10^{-9}
$CO_2(g)$	7.87×10^{-2}	7.88×10^{-2}
HCl(g)	2.83×10^{-6}	3.20×10^{-6}
$H_2(g)$	4.08×10^{-6}	2.25×10^{-9}
$H_2O(g)$	9.06×10^{-2}	9.07×10^{-2}
NO(g)	1.60×10^{-3}	1.06×10^{-4}
$NO_2(g)$	3.26×10^{-6}	1.25×10^{-6}
$N_2(g)$	7.39×10^{-1}	7.39×10^{-1}
NaCl(g)	8.51×10^{-7}	5.86×10^{-7}
NaOH(g)	2.86×10^{-6}	2.50×10^{-8}
$Na_2SO_4(l)$	---------	1.54×10^{-6}
$Na_2SO_4(g)$	1.68×10^{-11}	4.63×10^{-8}
O(g)	8.06×10^{-6}	3.98×10^{-9}
OH(g)	1.99×10^{-4}	1.49×10^{-6}
$O_2(g)$	8.13×10^{-2}	8.21×10^{-2}
$SO_2(g)$	8.51×10^{-5}	7.68×10^{-5}
$SO_3(g)$	4.40×10^{-7}	7.12×10^{-6}

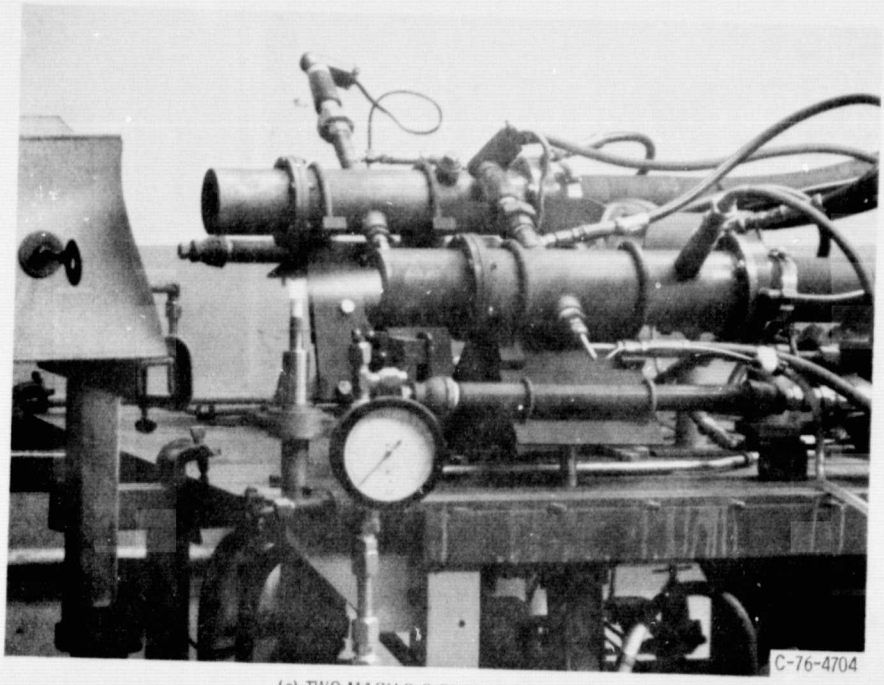

(a) TWO MACH 0.3 BURNER RIGS.

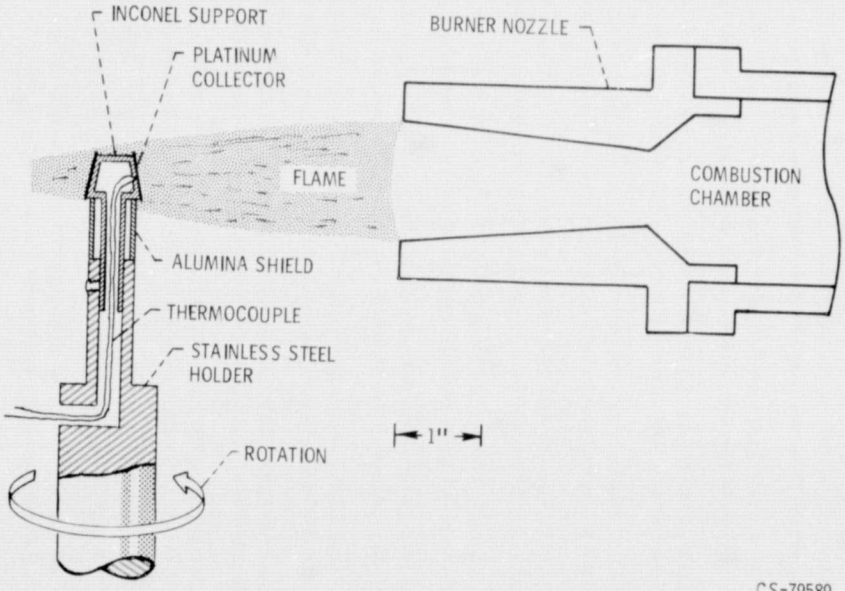

(b) SCHEMATIC.

Figure 1. - Burner-rig salt deposition apparatus.

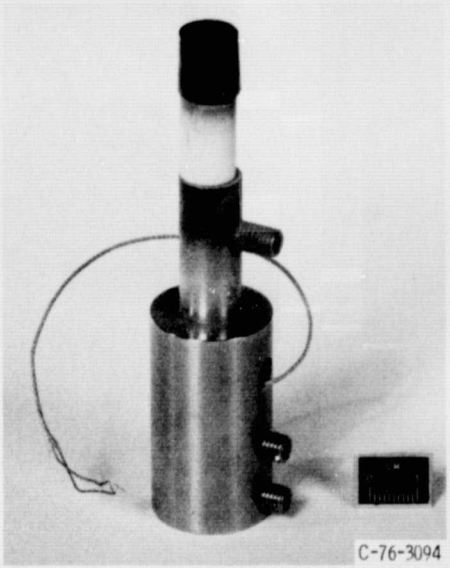

Figure 2. - Platinum collector assembly.

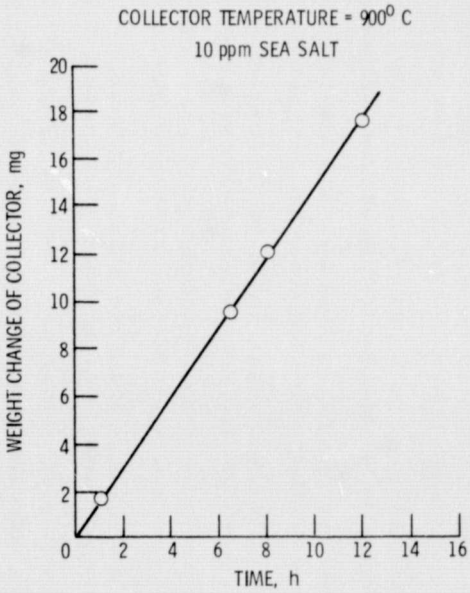

Figure 3. - Collector weight gain against time for sea salt-doped flame.

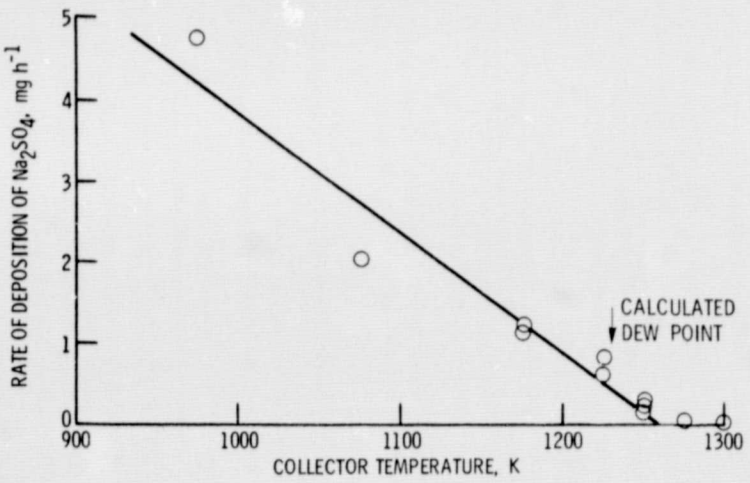

Figure 4. - Deposition of Na_2SO_4 from flame doped with 11.3 ppm sea salt.

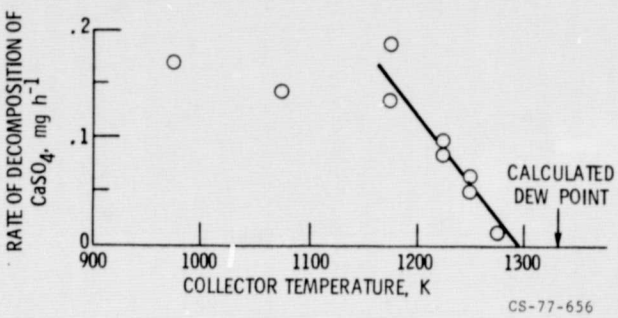

Figure 5. - Deposition of $CaSO_4$ from flame doped with 11.3 ppm sea salt.

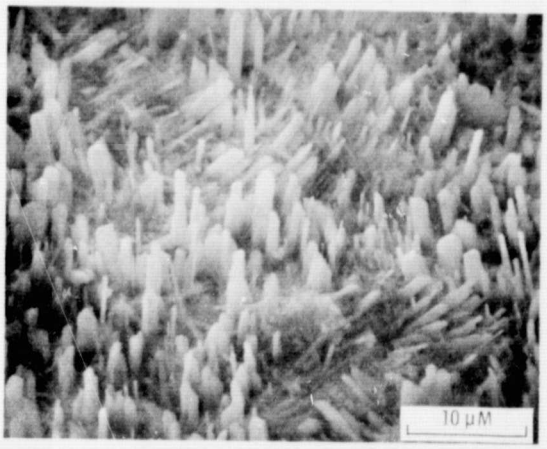

(a)

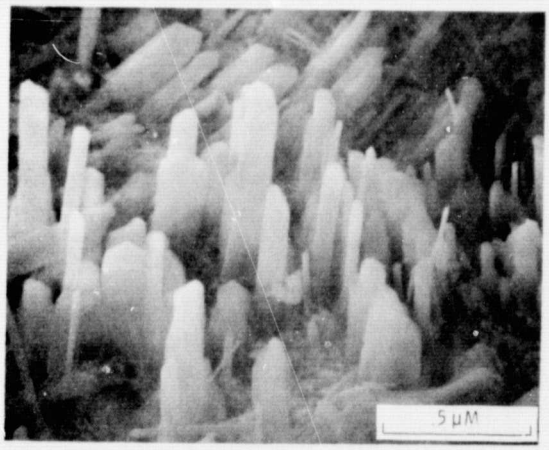

(b)

Figure 6. - SEM micrographs of deposit collected from flame doped with 11.3 ppm sea salt.

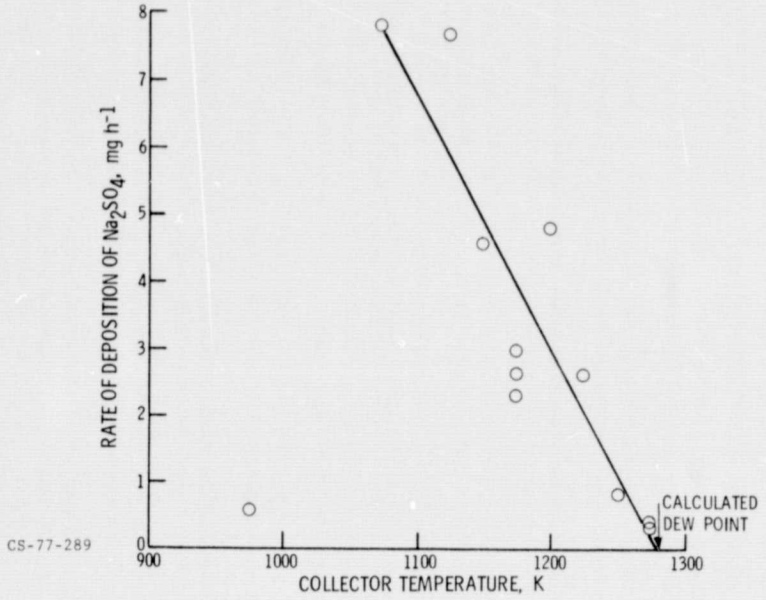

Figure 7. - Deposition of Na_2SO_4 from flame doped with 10.5 ppm Na_2SO_4.

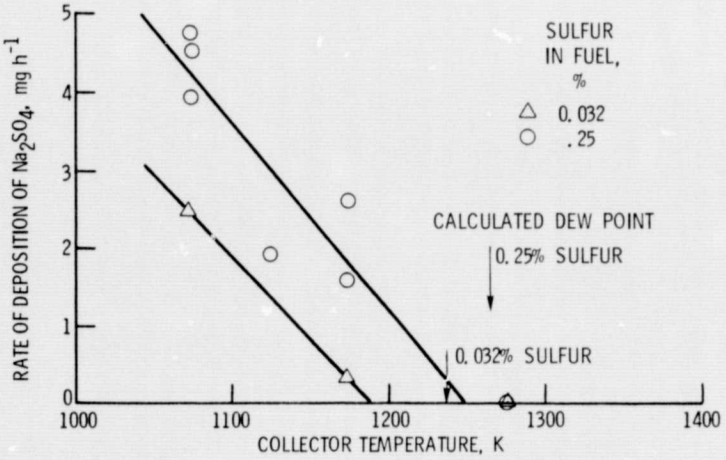

Figure 8. - Deposition of Na_2SO_4 from flame doped with 8.0 ppm NaCl.

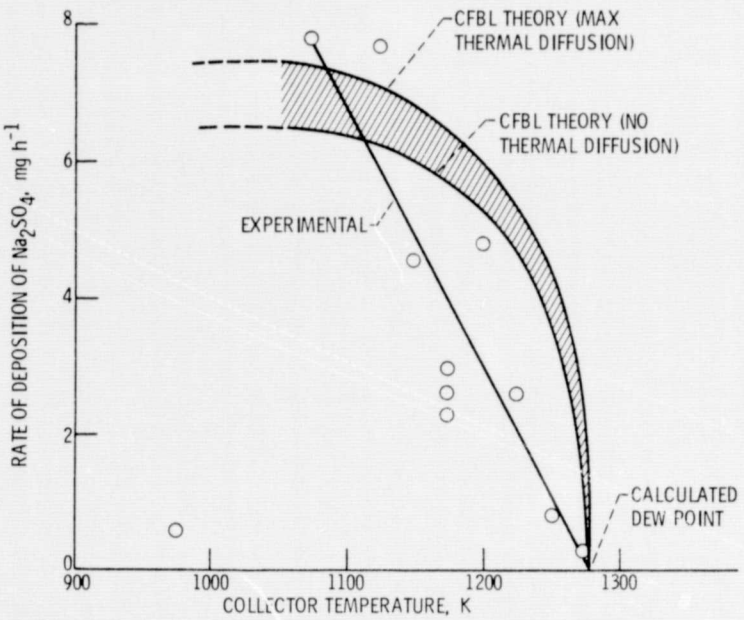

Figure 9. - Comparison of chemically frozen boundary layer (CFBL) theory (eqs. (1), (6)) with observed Na_2SO_4 deposition rate from Na_2SO_4 - seeded combustion products.

NASA-Lewis